New Water-Containing Phase Derived from the $Sr_3Fe_2O_{7-\delta}$ Phase of the Ruddlesden−Popper Structure

M. Matvejeff,[†,‡] M. Lehtimäki,[†] A. Hirasa,[†] Y.-H. Huang,[†] H. Yamauchi,[†] and M. Karppinen*,[†]

Materials and Structures Laboratory, Tokyo Institute of Technology, Yokohama 226-8503, Japan, and Laboratory of Inorganic and Analytical Chemistry, Helsinki University of Technology, FIN-02015 Espoo, Finland

Received January 18, 2005. Revised Manuscript Received March 4, 2005

Here a novel water-containing derivative phase (with the elongated *c* axis from 20.2 to 28.0 Å) is reported for the $n = 2$ member of the $Sr_{n+1}Fe_nO_{3n+1-\delta}$ Ruddlesden−Popper series, i.e., $Sr_3Fe_2O_{7-\delta}$ with the layer sequence of $SrO-SrO-FeO_2-SrO_{1-\delta}-FeO_2$. The intercalated water molecules in the derivative phase are believed to reside within the $(SrO)_2$ double-layer block, probably accompanied by additional protons. The latter belief is supported by the fact that upon water incorporation iron was found to be reduced (toward the trivalent state). High-quality samples of the parent $Sr_3Fe_2O_{7-\delta}$ phase were synthesized from a solution-derived precursor powder. For samples synthesized in air cerimetric titration yielded an oxygen content at $7 - \delta = 6.44$. More oxygen-deficient samples with $7 - \delta = 6.32$ and 6.18 were obtained by postannealing the as-synthesized material in flowing Ar gas at 400 and 500 °C, respectively. Independent of the value of δ, all the $Sr_3Fe_2O_{7-\delta}$ samples transformed to the water derivative when subjected to an ambient (humid) atmosphere, whereas the speed of the topotactic derivative-phase formation increased with increasing δ. On the other hand, reversible dehydration of the derivative phase occurred upon heating in two distinguishable steps below ∼230 °C.

Introduction

Among the functional multilayered transition-metal oxides, so-called Ruddlesden−Popper (RP)[1] phases with a nominal stoichiometry of $A_{n+1}T_nO_{3n+1}$ or $A_2Q_{n-1}T_nO_{3n+1}$ (A, Q = Sr, La, etc.; T = transition metal) form an interesting group of materials, as they possess relatively simple structures but exhibit a variety of spectacular properties ranging from high-T_c superconductivity[2−5] to colossal magnetoresistance.[6−8] The ideal crystal structure of an RP oxide may be described as the stacking of (A,Q)O layers and TO_2 planes along the crystallographic *c* axis into a perovskite $[(A,Q)TO_3]_n$ block which is separated from the adjacent perovskite block by an additional AO layer, resulting in a layer sequence of $AO-AO-TO_2-[(A,Q)O-TO_2]_{n-1}$. The additional AO layer causes the successive $AO-AO-TO_2-[(A,Q)O-TO_2]_{n-1}$ structural units to be translated by $^1/_2$ in the [110] direction of the primitive tetragonal unit cell. The resultant *c*-axis-elongated unit cell possesses body-centered symmetry and contains two $A_{n+1}T_nO_{3n+1}$ or $A_2Q_{n-1}T_nO_{3n+1}$ formula units.

Like perovskite-derived oxides in general, the RP oxides commonly exhibit oxygen deficiency/nonstoichiometry, especially within their (A,Q)O layers in the perovskite block. On the other hand, the rock-salt-type $(AO)_2$ double layer is flexible enough to accommodate additional structural layers of various types. Such characteristics are well manifested by the multilayered copper oxides of the general formula $M_mA_2Q_{n-1}Cu_nO_{m+2+2n\pm\delta}$ and the layer sequence $AO-(MO_{1\pm\delta/m})_m-AO-CuO_2-(Q-CuO_2)_{n-1}$, i.e., phases with completely oxygen-deficient Q cation layers between the CuO_2 planes in the perovskite block and an extra $(MO_{1\pm\delta/m})_m$ "charge-reservoir block" between the two AO layers.[9] Among the $M_mA_2Q_{n-1}Cu_nO_{m+2+2n\pm\delta}$ superconductors, the parent RP ($m = 0$ or "zero") phases are rather special.[5,9] Most profoundly, the $n = 3$ member of the $Ba_2Ca_{n-1}Cu_nO_{2+2n\pm\delta}$ "homologous series", i.e., $Ba_2Ca_2Cu_3O_{8\pm\delta}$ ($T_c \approx 125$ K), which can be obtained by means of ultra-high-pressure synthesis only, instantaneously accommodates water between the two rock-salt-type BaO layers when exposed to (humid) air.[10] The water intercalation results in the formation of a well-defined derivative phase with an elongated *c* axis lattice parameter (from 28.3 to 34.0 Å per two formula units). This "watery" derivative is also a superconductor with $T_c \approx 90$ K.[10] Interestingly, wet-chemical redox analysis has revealed that the parent $Ba_2Ca_2Cu_3O_{8\pm\delta}$

* To whom correspondence should be addressed. E-mail: karppinen@msl.titech.ac.jp.
† Tokyo Institute of Technology.
‡ Helsinki University of Technology.

(1) Ruddlesden, S. N.; Popper, P. *Acta Crystallogr., Sect. A* **1957**, *10*, 538; **1958**, *11*, 54.
(2) Bednorz, J. G.; Müller, K. A. *Z. Phys. B* **1986**, *64*, 189.
(3) Adachi, S.; Yamauchi, H.; Tanaka, S.; Môri, N. *Physica C* **1993**, *208*, 226; *212*, 164.
(4) Hiroi, Z.; Takano, M.; Azuma, M.; Takeda, Y. *Nature (London)* **1993**, *364*, 315.
(5) Yamauchi, H.; Karppinen, M. *Physica C* **2000**, *335*, 273.
(6) Von Helmolt, R.; Wecker, J.; Holzapfel, B.; Schultz, L.; Samwer, K. *Phys. Rev. Lett.* **1993**, *71*, 2331.
(7) Moritomo, Y.; Asamitsu, A.; Kuwahara, H.; Tokura, Y. *Nature (London)* **1996**, *380*, 141.
(8) Tokura, Y. *Phys. Today* **2003**, *56* (7), 50.
(9) Karppinen, M.; Yamauchi, H. *Mater. Sci. Eng., R* **1999**, *26*, 51.
(10) Hosomi, T.; Suematsu, H.; Fjellvåg, H.; Karppinen, M.; Yamauchi, H. *J. Mater. Chem.* **1999**, *9*, 1141.

10.1021/cm050106z CCC: $30.25
Published on Web 04/19/2005

phase is more strongly oxidized than its water derivative.[11] Since accommodation of neutral H_2O molecules should not change the valence state of copper, it was suggested that upon the H_2O intercalation additional protons could be incorporated into the structure as well. Later it was revealed that the $n = 2$ and 4 members of the same $Ba_2Ca_{n-1}Cu_nO_{2+2n\pm\delta}$ series undergo parallel topotactic water-intercalation processes.[12]

Among the $n = 1$ RP oxides, i.e., A_2TO_4, water derivatives have been reported for Ba_2ZrO_4[13] and $NaEuTiO_4$.[14] In the latter phase, the A-site cations Na and Eu are ordered for the structure to repeat the layer sequence of NaO−NaO−TiO_2−EuO−EuO−TiO_2, and the incorporated water goes exclusively into the $(NaO)_2$ portion of the structure. Upon water intercalation the *c* parameter increases from 12.5 to 15.1 Å, i.e., 2.6 Å per water-containing $(NaO)_2$ block.[14]

Recently water-containing derivatives were also reported for the $n = 3$ RP iron oxides of $Sr_3LaFe_3O_{10-\delta}$[15] and $Sr_3NdFe_3O_{10-\delta}$.[16] Parallel to the aforementioned cases, the phase transformation occurs as a topotactic insertion of water molecules between the two adjacent (Sr,La/Nd)O layers upon exposure to ambient air. In the present work, we reveal a similar behavior for the $n = 2$ RP iron oxide $Sr_3Fe_2O_{7-\delta}$. The derivative-phase formation is moreover shown to strongly depend on the oxygen-vacancy concentration, δ, and result in significant reduction in the valence state of iron. It should be noted that in some of the early works the somewhat weak phase stability of $Sr_3Fe_2O_{7-\delta}$ was indeed recognized,[17,18] but no attention was paid to the phase-degradation product(s).

Experimental Section

The master sample of the parent $Sr_3Fe_2O_{7-\delta}$ phase was synthesized using a liquid-based EDTA complexing method that allowed us to obtain a highly homogeneous precursor mixture and hence to realize the synthesis of well-crystallized single-phase samples at relatively low temperatures. This is especially important for the present iron oxide, which requires very high synthesis temperatures, if prepared through conventional solid-state synthesis from carbonates/oxides. Stoichiometric amounts of $Sr(NO_3)_2$ and $Fe(NO_3)_3 \cdot 9H_2O$ were dissolved in distilled water, together with EDTA, aided by magnetic stirring. The (molar) quantity of EDTA was 1.2 times of that of the precursor nitrates. The resulting dark red solution was evaporated in a hot-water bath overnight, and the resultant dry gel was decarbonated in an electric furnace at 450 °C for 3−4 h. This intermediate product was calcined in air at 1000 °C for ca. 110 h with three intermediate grindings. The final product was large-grained and dark gray in color. The high degree of crystallization was evident from the strong metallic luster not seen in the samples prepared through conventional solid-state synthesis routes. The as-synthesized sample was confirmed to be of the single $Sr_3Fe_2O_{7-\delta}$ phase by powder X-ray diffraction (XRD; Rigaku RINT2550VK/U equipped with a rotating anode, Cu Kα radiation, 2θ range 3.0−120.0°, scanning step 0.02°, scanning speed 6 deg/min). Here it should be emphasized that special attention was paid not only to use a fast measurement program but also to minimize the time for preparing the XRD specimen from the sample immediately after its removal from the furnace.

Table 1. Oxygen Content, $7 - \delta$, Fe Valence, *V*(Fe), and Lattice Parameters *a* and *c* for the Three $Sr_3Fe_2O_{7-\delta}$ Samples (of the Parent RP Structure) Synthesized in the Present Study[a]

sample	$7 - \delta$	*V*(Fe)	*a* (Å)	*c* (Å)
as-air-synthesized	6.44(1)	3.44(1)	3.866(0.3)	20.173(2)
400 °C-Ar-annealed	6.32(1)	3.32(1)	3.873(0.3)	20.176(2)
500 °C-Ar-annealed	6.18(1)	3.18(1)	3.881(0.5)	20.153(3)

[a] The error estimates/standard deviations are given in parentheses.

Portions of the master sample of $Sr_3Fe_2O_{7-\delta}$ were also subjected to subsequent heat treatments for oxygen-content control. From preliminary experiments it was found that upon annealing in oxidizing conditions (1−140 atm of O_2, 350−450 °C) the oxygen content of the phase remained essentially unchanged, whereas postannealings in an inert atmosphere (Ar or N_2) resulted in considerable oxygen losses. Hence, for the present study, besides the as-air-synthesized sample, two Ar-annealed samples were prepared at 400 and 500 °C. (Attempts to prepare more strongly reduced samples at the higher temperatures of 550 and 600 °C resulted in decomposition of the phase.) For both annealings, the annealing period was 16 h and the annealing was followed by quenching to room temperature and immediate characterization. If storing was necessary, the samples were kept at 250 °C in a box furnace in air. (Note that storing samples at higher temperatures would result in reoxygenation of the phase, as was concluded from preliminary thermogravimetric (TG) measurements carried out in O_2 gas, whereas storing at room temperature in air would result in transformation into the water-containing phase.)

The precise Fe valence/oxygen content was determined for the samples by several parallel cerimetric titrations with reproducibility better than ±0.01. To investigate the thermal stability and the amount of intercalated water, TG experiments were carried out for some of the air-exposed samples using two different thermobalances (Perkin-Elmer Pyris 1 and MAC Science TG/DTA 2000S). The sample amount was ∼30 mg, and the thermograms were recorded in O_2 using a heating rate of 2 °C/min.

Magnetic properties of the samples were measured using a SQUID magnetometer (Quantum Design MPMS-XL) with an applied magnetic field of 10 Oe.

Results and Discussion

Precise oxygen contents for the as-air-synthesized and the two Ar-annealed samples of $Sr_3Fe_2O_{7-\delta}$ are given in Table 1 together with corresponding Fe valence values and lattice parameters *a* and *c*. Even the as-synthesized sample was found strongly oxygen-deficient; i.e., $\delta = 0.56$. At the same time, iron is at a relatively high (average) valence state of 3.44. A Rietveld refinement of the X-ray diffraction data (Figure 1a) carried out in space group *I*4/*mmm* located the oxygen vacancies in the single SrO layer between the two FeO_2 planes in the perovskite block, being in agreement with previous results.[18] The determined value of 0.56 for δ

(11) Karppinen, M.; Hosomi, T.; Yamauchi, H. *Physica C* **2002**, *382*, 276.
(12) Karppinen, M.; Yamauchi, H.; Hosomi, T.; Suematsu, H.; Fjellvåg, H. *J. Low Temp. Phys.* **1999**, *117*, 843. Yamauchi, H.; Karppinen, M.; Hosomi, T.; Fjellvåg, H. *Physica C* **2000**, *338*, 38.
(13) Shpanchenko, R. V.; Antipov, E. V.; Kovba, L. M. *Mater. Sci. Forum* **1993**, *133*−*136*, 639.
(14) Toda, K.; Kameo, Y.; Kurita, S.; Sato, M. *Bull. Chem. Soc. Jpn.* **1996**, *69*, 349.
(15) Nishi, T.; Toda, K.; Kanamaru, F.; Sakai, T. *Key Eng. Mater.* **1999**, *169*−*170*, 235.
(16) Pelloquin, D.; Hadermann, J.; Giot, M.; Caignaert, V.; Michel, C.; Hervieu, M.; Raveau, B. *Chem. Mater.* **2004**, *16*, 1715.
(17) Gallagher, P. K.; MacChesney, J. B.; Buchanan, D. N. E. *J. Chem. Phys.* **1966**, *45*, 2466.
(18) Dann, S. E.; Weller, M. T.; Currie D. B. *J. Solid State Chem.* **1992**, *97*, 179.

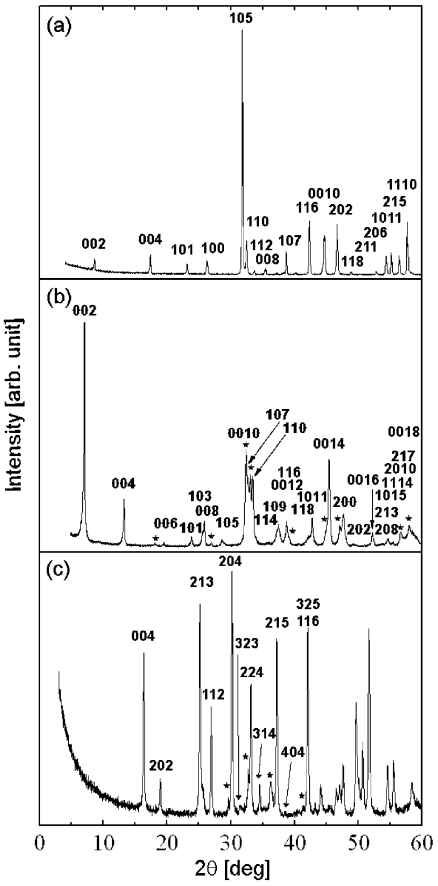

Figure 1. XRD patterns for (a) as-air-synthesized ($\delta = 0.56$), (b) air-exposed (74 h), and (c) water-dipped $Sr_3Fe_2O_{7-\delta}$ samples. The indexes in (a) are for the RP $Sr_3Fe_2O_{7-\delta}$ phase (*I*4/*mmm*, $a = 3.86$ Å, $b = 20.17$ Å), in (b) for the structure model shown in Figure 2 for the water-derivative phase (*I*4/*mmm*, $a = 3.82$ Å, $b = 28.03$ Å), and in (c) for the cubic $Sr_3Fe_2(OH)_{12}$ phase (*Ia*$\bar{3}$*d*, $a = 13.2$ Å).[18] Asterisks in (b) are for the peaks due to the parent $Sr_3Fe_2O_{7-\delta}$ phase and in (c) for the peaks due to the $SrCO_3$ impurity.

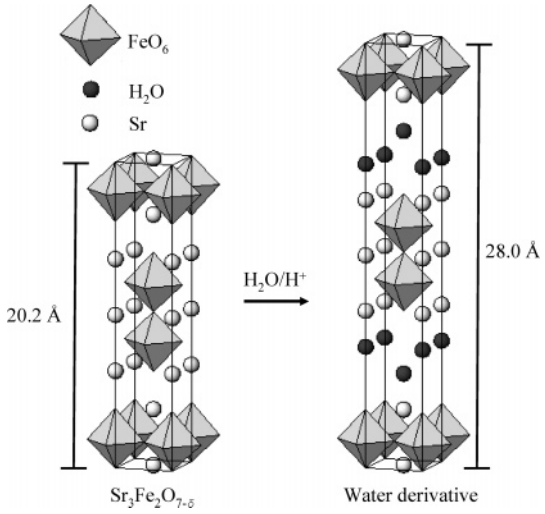

Figure 2. Schematic illustration of the crystal structures of the $Sr_3Fe_2O_{7-\delta}$ phase and its layered water-derivative phase.

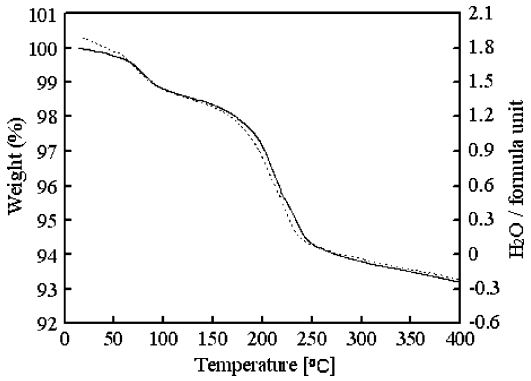

Figure 3. Thermogravimetric curves recorded with two different TG instruments (Perkin-Elmer, MAC Science) in O_2 with a heating rate of 2 °C/min for an air-exposed $Sr_3Fe_2O_{7-\delta}$ specimen that according to XRD contains a significant amount of the derivative phase.

corresponds to a situation in which roughly half of the iron atoms in the FeO_2 planes have 5-fold pyramidal coordination and the other half 6-fold octahedral coordination. Upon annealing the as-synthesized sample in Ar gas at 400 and 500 °C, the amount of oxygen vacancies increased to $\delta = 0.68$ and 0.82, respectively. With decreasing oxygen content, the lattice parameter *a* increased, whereas the parameter *c* slightly decreased (Table 1). These changes in the lattice parameters with decreasing oxygen content are exactly what one would expect for a system in which the number of the larger Fe^{III} species increases at the expense of the smaller, Jahn−Teller-distorted Fe^{IV} species.

When subjected to ambient atmosphere, all the $Sr_3Fe_2O_{7-\delta}$ samples (independent of the value of δ) were found to transform to another presumably layered phase within a couple of hours of exposure. Here, taking an analogy to water intercalation in various RP phases as discussed in the Introduction, we expect that the presently discovered derivative of the $Sr_3Fe_2O_{7-\delta}$ phase has accommodated water within the $(SrO)_2$ double-layer block (Figure 2). In the present case, the room temperature topotactic transformation of the parent RP phase to the (water-containing) derivative may be best evidenced by the appearance of a new low-angle diffraction peak at about 6.2°; see Figure 1b. At the same time, the (002) reflection of the parent RP phase at about 8.6° practically disappears. The crystal structure of the new water-containing phase was satisfactorily refined in space group *I*4/*mmm*:[15] peaks that were nonexplainable by the assumed structure model were all found to be due to the parent $Sr_3Fe_2O_{7-\delta}$ phase (marked with an asterisk in Figure 1b) yet present to some extent (approximately 10−15%) in the "fully" air-exposed samples. The lattice parameters obtained for the water derivative are $a = 3.822(0.4)$ Å and $c = 28.029(4)$ Å. Hence, we may conclude that upon the phase change the lattice expands along the *c* axis direction by 7.8 Å (= 28.0 − 20.2 Å) per two formula units. That is, for $Sr_3Fe_2O_{7-\delta}$ the lattice expansion per "watery layer" is 3.9 Å, being comparable to those reported for other RP systems: 2.6 Å for $(NaO)_2$ in $NaEuTiO_4$,[14] 2.9 Å for $(BaO)_2$ in $Ba_2Ca_{n-1}Cu_nO_{2+2n\pm\delta}$ ($n = 2-4$),[10,12] 3.4 Å for $[(Sr,Nd)O]_2$ in $Sr_3NdFe_3O_{10-\delta}$,[16] and 3.9 Å for $[(Sr,La)O]_2$ in $Sr_3LaFe_3O_{10-\delta}$.[15]

To gain further evidence to support the proposed water-intercalation scheme, we performed TG measurements for samples which according to XRD data contained significant amounts of the derivative phase. In Figure 3 are shown two representative TG curves recorded for the same sample but with different equipment (to demonstrate the excellent reproducibility). Two distinct weight-loss steps, presumably due to release of water, are seen at about 80 and 200 °C, in

evident resemblance to the observations by Nishi et al.[15] and Pelloquin et al.[16] for the watery derivatives of their Fe-based $n = 3$ RP phases. It should be emphasized that beyond 250 °C no further weight-loss steps were seen. This fact rules out the possibility of our water-derivative phase containing carbonate groups. (We expect the possible CO_2 evolution to occur in the temperature range from ∼500 to ∼1000 °C; see, e.g., the case of the related $Sr_4Fe_2O_6CO_3$ phase.[19]) The reversibility of the phase transformation was confirmed by heating several of the derivative-phase-containing samples in air at 350 °C: these heat treatments always resulted in samples with diffraction patterns that were essentially identical to that of the parent phase, though no detailed structure analyses were done due to the relatively low crystallinity of the dehydrated samples. We also recognize the possibility[15,16] that the pseudoplateau seen in the TG curves at about 100−150 °C might correspond to another intermediate water-containing derivative phase, though this is not verified within the scope of the present work.

As estimated from the TG data the overall water content in our air-exposed $Sr_3Fe_2O_{7-\delta}$ samples was around 1.8 H_2O molecules per formula unit (Figure 3), whereas for the $n = 3$ phases the presence of two H_2O molecules per formula unit was reported.[15,16] The somewhat lower overall water content in our case may be attributed to the fact that according to the XRD data the air-exposed samples always contained traces of the parent phase. In other words, even though the first signs of the derivative phase appeared in the diffraction pattern in the fastest case even within a few tens of minutes of exposure to ambient air, some indication of the presence of the parent phase remained even after weeks of air exposure. Anticipating that the derivative-phase formation is accelerated by increasing humidity, we kept some specimens of the parent-phase samples in saturated humidity, i.e., in a box with water at the bottom, and dipped other specimens in distilled water. The two treatments, however, both resulted in the formation of not the layered derivative phase but a water-containing phase whose diffraction pattern (Figure 1c) is readily indexed according to the cubic crystal lattice ($Ia\bar{3}d$, $a = 13.2$ Å) as previously reported for "$Sr_3Fe_2(OH)_{12}$".[20] Samples with larger amounts of the cubic phase were brown-red in color, suggesting the presence of a large amount of trivalent iron. Note also that $Sr_3Fe_2(OH)_{12}$ readily reacts with carbon dioxide, explaining why a trace of $SrCO_3$ was always seen in the diffraction patterns for $Sr_3Fe_2(OH)_{12}$ (Figure 1c).

The speed of the derivative-phase formation was investigated with respect to the oxygen-vacancy concentration of the parent phase by subjecting specimens of the three $Sr_3Fe_2O_{7-\delta}$ compositions of $\delta = 0.56$, 0.68, and 0.82 all at once to the ambient atmosphere and recording their XRD patterns in terms of the air-exposure time. In parts a−c, respectively, of Figure 4 time evolution of the 6.2° diffraction peak that is characteristic of the derivative phase is shown for the three $Sr_3Fe_2O_{7-\delta}$ specimens. It is seen that as the degree of oxygen nonstoichiometry, δ, increases the phase transformation to the *c*-axis-elongated derivative phase becomes much faster.

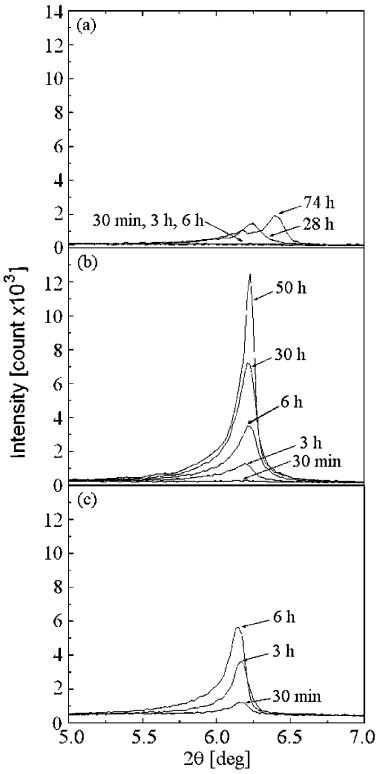

Figure 4. Derivative-phase formation as followed through the development of the low-angle diffraction peak at about 6.2° in the XRD patterns recorded for (a) as-air-synthesized ($\delta = 0.56$), (b) 400 °C-Ar-annealed ($\delta = 0.68$), and (c) 500 °C-Ar-annealed ($\delta = 0.82$) $Sr_3Fe_2O_{7-\delta}$ samples in terms of the air-exposure time.

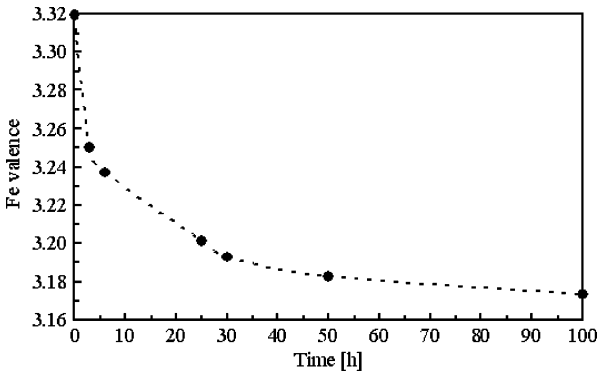

Figure 5. Gradual changes in the (average) valence of iron (caused by an increase in the relative amount of the derivative phase) for the sample with an initial composition of $Sr_3Fe_2O_{7-\delta}$ ($\delta = 0.68$) in terms of the air-exposure time. The broken line is a guide to the eyes.

An important observation with respect to the valence state of iron could be made from the cerimetric titration experiments, carried out for a $\delta = 0.68$ sample in terms of the time after its exposure to ambient air was started (Figure 5). As the air-exposure time increased, i.e., the relative amount of the derivative phase increased, the average valence of iron decreased. Taking an analogy to the case previously reported for $Ba_2Ca_2Cu_3O_{8\pm\delta}$,[11] this may be considered as an indication that not only neutral H_2O molecules but also positively charged particles—presumably H^+/H_3O^+ species—are incorporated into the $Sr_3Fe_2O_{7-\delta}$ structure upon formation of the derivative phase. (Here it is also worthwhile to refer to the

(19) Yamaura, K.; Huang, Q.; Lynn, J. W.; Erwin, R. W.; Cava, R. J. *J. Solid State Chem.* **2000**, *152*, 374.
(20) Nevskii, N. N.; Ivanov-Emin, B. N.; Nevskaya, N. A.; Kaziev, G. Z.; Belov, N. V. *Dokl. Akad. Nauk SSSR* **1982**, *264*, 857.

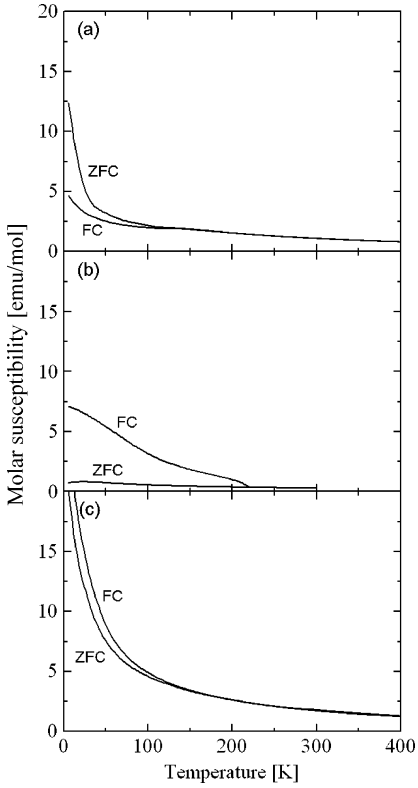

Figure 6. Molar magnetic susceptibility versus temperature for the (a) as-air-synthesized $Sr_3Fe_2O_{7-\delta}$ ($\delta = 0.56$) sample, (b) water-derivative sample (obtained from $Sr_3Fe_2O_{6.44}$ after 74 h of air exposure), and (c) "$Sr_3Fe_2(OH)_{12}$"-phase sample (obtained from $Sr_3Fe_2O_{6.44}$ through water-dipping).

newly discovered watery CoO_2-layer-based superconductor $Na_xCoO_{2-\delta}\cdot yH_2O$[21] as the presence of excess protons/oxonium ions has been proposed for this layered phase too.[22,23]) Hence, the driving force for the water intercalation is likely to be the strong tendency for the RP oxides (which involve high-valent 3d cations such as Cu^{III} and Fe^{IV}) to be reduced, whereas the positive impact of the increasing amount of oxygen vacancies for the derivative-phase formation (also revealed in the present study) may just be an indication that oxygen vacancies enhance the kinetics of the intercalation process. It is also tempting to use the wet-chemical redox analysis and TG data for our air-exposed $\delta = 0.68$ sample (of approximately 85−90% phase purity in terms of the derivative phase) to estimate the Fe valence (~3.1 from Figure 5) and water content (~2 molecules per formula unit from Figure 3) values for the (pure) derivative phase. Using these values, we propose the following chemical formula for our novel water-derivative phase (obtained from $Sr_3Fe_2O_{6.3}$): $Sr_3Fe_2O_{6.3}(H_3O)_{0.4}\cdot 1.6H_2O$ or $Sr_3Fe_2O_{5.9}(OH)_{0.4}\cdot 2H_2O$.

We also characterized the samples for their magnetic property. The data are shown in Figure 6. In accordance with previous reports for $Sr_3Fe_2O_{7-\delta}$,[24,25] our as-air-synthesized $Sr_3Fe_2O_{6.44}$ sample shows branching of the zero-field-cooled (ZFC) and field-cooled (FC) curves as an indication of the paramagnetic-to-antiferromagnetic transition at about 140 K (Figure 6a). The new water-derivative phase behaves somewhat differently: it shows a transition to a canted antiferromagnetic state at about 220 K (Figure 6b). The sample obtained from $Sr_3Fe_2O_{6.44}$ through water-dipping remains paramagnetic down to 4 K (Figure 6c), as previously reported for the $Sr_3Fe_2(OH)_{12}$ phase.[26] Hence, the parent RP phase $Sr_3Fe_2O_{7-\delta}$ and its two water derivatives all exhibit different magnetic characteristics.

In conclusion, we have obtained a novel water-containing derivative of a layered structure from an $n = 2$ Ruddlesden−Popper compound, $Sr_3Fe_2O_{7-\delta}$. Intercalation of water in $Sr_3Fe_2O_{7-\delta}$ has been revealed to be accompanied by expansion of the c axis lattice parameter by 3.9 Å per formula unit and also by reduction in the valence state of iron in the FeO_2 planes.

Acknowledgment. This work was supported by Grants-in-Aid for Scientific Research (Nos. 15206002 and 15206071) from the Japan Society for the Promotion of Science. M.M. acknowledges financial support from the Finnish Cultural Foundation and Scandinavia-Japan Sasakawa Foundation.

CM050106Z

(21) Takada, K.; Sakurai, H.; Takayama-Muromachi, E.; Izumi, F.; Dilanian, R. A.; Sasaki, T. *Nature (London)* **2003**, *422*, 53.
(22) Karppinen, M.; Asako, I.; Motohashi, T.; Yamauchi, H. *Chem. Mater.* **2004**, *16*, 1693.
(23) Takada, K.; Fukuda, K.; Osada, M.; Nakai, I.; Izumi, F.; Dilanian, R. A.; Kato, K.; Takata, M.; Sakurai, H.; Takayama-Muromachi, E.; Sasaki, T. *J. Mater. Chem.* **2004**, *14*, 1448.
(24) Adler, P. *J. Solid State Chem.* **1997**, *130*, 129.
(25) Kuzushita, K.; Morimoto, S.; Nasu, S.; Nakamura, S. *J. Phys. Soc. Jpn.* **2000**, *69*, 2767.
(26) Okamoto, S. *Yogyo Kyokaishi* **1982**, *90* (1), 30.